Particle Accelerators
1973, Vol. 5, pp. 23-44

TENTATIVE DESIGNS FOR A STORAGE RING FOR IMPROVING THE DUTY FACTOR OF A 40-MeV ELECTRON LINAC

C. H. WESTCOTT
Accelerator Physics Branch, Atomic Energy of Canada Limited,
Chalk River Nuclear Laboratories, Chalk River, Ontario, Canada

In amplification of a brief conference report[1] the present paper gives details of a design for a storage ring for duty-factor improvement of the beam of an ~40-MeV electron linac. Such linacs have typically a duty factor of ~0.1%, and Knowles[2] has shown that the research programme, based on such a linac, could be considerably broadened if the duty factor could be raised to near unity (say 60 to 95%) without increasing the mean current. By contrast with prior proposals at higher energy,[3,4] simplicity and relatively low cost are achieved in the present designs at the price of restricting the spread of energy ΔE of the stored electrons to $\Delta E/E \approx 0.1$–0.15%, this being acceptable for the experiments proposed.

In order to examine how the linac beam emittance available and the energy range to be stored may influence the design, four alternative tentative ring designs are presented. Factors which may influence the final choice of design for a particular installation are also discussed in relation to the practical limitations of available components.

1. INTRODUCTION

The proposal[5] for a duty-factor improving storage ring for ~ 40 MeV electrons from a linac, which originated in connection with the University of Toronto linac, using estimates of the beam emittance appropriate to that linac, is now presented in general terms as a study aiming at a relatively modest ring, having only 31 principal components, whose specification could be completed with only a minimum of preliminary experimental development of special units; the points where further study would be required are also discussed. The first two designs[5] differed in the specification for the incoming beam emittance and were for an energy range of $\Delta E/E = 0.1\%$. Two additional designs, for $\Delta E/E = 0.15\%$ are also described below. The two original alternative designs have also been studied[6] from the point of view of tolerances both on mechanical alignment and on field-strengths of the ring components. The results derived in Ref. 6 are summarized below, together with the space-charge and instability limits on beam intensity which are taken from the same document.

Of the variants of the older designs[5] the value $\beta = 0.475$ has now been selected, β being the second-order field index of the bending magnets (n, the first-order index, being 0.5). With this choice these rings give a satisfactory achromatic performance, the extraction of the electrons from the ring being substantially simultaneous for all the electron energies within the range accepted for storage, although they are not designs which are inherently achromatic.† The present designs, like their predecessors[3,4] remain theoretical, but from a comparison of our 0.1% and 0.15% alternatives, it is felt that any designs for $\Delta E/E \cong 0.2\%$ or more should probably be based on the alternative approach of the Saskatoon[3,4] studies. For our rings a preliminary study was undertaken of the effects of imperfections in components (e.g. the 6th and 10th harmonics in quadrupoles), these being emphasized because we expect to need quadrupoles with effective lengths (for the worst cases) of only about 1.7 times their bore. The cost of the ring is sensitive to its aperture so that the factors just mentioned, together with the exactness of position of the beam spot and how well the beam can be cut off at the desired energy limits must define the choice of a design. For the latter factor this is because energy 'tails' may result in electrons striking ring components (e.g. hitting the injection septum on subsequent turns), causing physical or radiation damage or unacceptable levels of radioactivity.

† In the Saskatoon[4] and ALIS[3] designs the injection and ejection septa were located in achromatic straight sections so that the closed orbit locations at these points were independent of the electron energy. For our rings this was not required.

It is because the characteristics of the linac beam to be used are crucial that the present paper presents alternative designs. The larger emittances assumed for two of the four rings described may be regarded as allowing something for possible drift (of the order of 0.5 mm) in the beam spot position, although it is hoped to reduce this to less than 0.1 mm in either plane, using a servo system if necessary, to minimize the cost and aperture of the ring.

2. GENERAL DESCRIPTION OF OPERATION AND STRUCTURE USED

The general mode of operation follows that of the Saclay ALIS[3] and the Saskatoon[4] ring proposals, viz., multi-turn 'coupled' injection into a storage ring and slow extraction using the method of 'one-third' resonance, i.e. ν_x (the number of radial betatron wavelengths per orbit) approaching a value $n/3$ where n is an integer not a multiple of 3—for our design $n = 7$. The basic structure of the ring is shown in Fig. 1, supplemented by Appendix I. It includes four 90° ($n = \frac{1}{2}$) bending magnets and sixteen 'fixed' magnetic quadrupoles; two sextupoles (H on figure, the alternative term being 'hexapole') provide the nonlinear terms which excite the one-third resonance extraction action. The 'pulsed' quadrupoles, which may be electrostatic, are used to vary the tuning i.e. ν_x, of the ring, and so to control the cycle of operation (Fig. 2). For general discussions of how these processes operate, see Refs. 3 and 4 and the many papers cited therein, as well as Refs. 5 and 6. The injection is 'coupled' in the sense that both radial (x-plane) and vertical (z-plane) betatron oscillations are excited, allowing a 5-turn injection, and also yielding a beam 'hollow' in x phase-space (cf. Fig. 4(b)) to facilitate extraction. Thus extraction occurs in the horizontal (x) plane, while injection perturbators operate in the z-(vertical) plane. The injection septum and the immediately preceding section of beam transport required should form an achromatic double bend to displace the beam vertically into the plane of the ring. The exit channel for the beam is in the plane of the ring and the extraction is outwards, but this channel has not yet been specified, since it depends on layout at the site.

The Twiss-matrix α- and β-functions and the momentum compaction factors $g(s)$† are important for the design. The β_x, β_z and g functions for the proposed first alternative ring are shown in Fig. 3; in fact these functions differ very little between our four alternative rings.

The specifications and constants of the four ring designs are collected in Table I and Appendix I. The $\beta = 0.475$ versions of the two designs of Ref. 5 are included, with for the first case some trivial adjustments; the new ($\Delta E/E = 0.15\%$) alternatives also use $\beta = 0.475$. The principal differences between these alternatives, apart from the $\Delta E/E$ chosen, arise from the incoming beam specifications (upper 4 lines of Table I). Those quantities which are the same for all rings or for three of them are given in Table A-I in the Appendix cited. For rings (2) and (3) a rather small emittance for the linac beam is assumed; we discuss in Sec. 7 below the larger emittance value used for ring (1) and the (roughly equivalent) assumption made for ring (4) of the smaller emittance with an allowance for a possible drift in the incoming beam-spot position. The differences in $\Delta E/E$ assumed have already been mentioned. Some other variations between these designs are also briefly discussed in Appendix I, e.g., the injection septum was larger for the first ring, in which a 15 mm orbit perturbation was used (cf. Fig. 13(b) for the specifications of these dimensions).

The resonant mode of extraction of the electrons from the ring is the crucial feature of the system. Injection occurs over five turns (365 nsec, the orbit period at 37 MeV being 73 nsec) while ejection must occur substantially uniformly over about 19,000 turns (this may fall to say $\sim 12{,}000$ turns if a duty factor of as low as 65% has to be tolerated). The recurrence rate of the Toronto linac ($720\ s^{-1}$) is assumed. The designs aim at having the stored electrons of all energies within the ΔE range simultaneously ejected; this is obtained by choosing $\beta = 0.475$ for the bending magnets.

† The notations used are for those of Bruck,[7] also used in the studies cited [3,4] of similar prior projects. s is a distance measured along the orbit, and g is a function of s; the average of g within the bending magnets of the ring is the 'overall' momentum compaction factor α (its reciprocal is sometimes quoted). Note that the more common $\beta(=v/c)$ must be distinguished from the Twiss $\beta_x(s)$ and $\beta_z(s)$ and from the β used as second-order magnet field gradient index (see, for example, page 222 of Livingood[8]).

The ejection is due to the sextupoles giving a non-linear term in the equations of motion (cf. Refs. 4, 5 and 6) and for ν_x near the resonant $2\frac{1}{3}$ value, we obtain in the x-phase-plane a stability triangle as shown in Fig. 4(a). The vertices of this triangle represent an amplitude of motion such that the effective ν_x, including the nonlinearity effects, is exactly on resonance, so that outside the triangle the particle motions are unstable. The nearer the 'tuning' of ν_x (calculated for small-amplitude

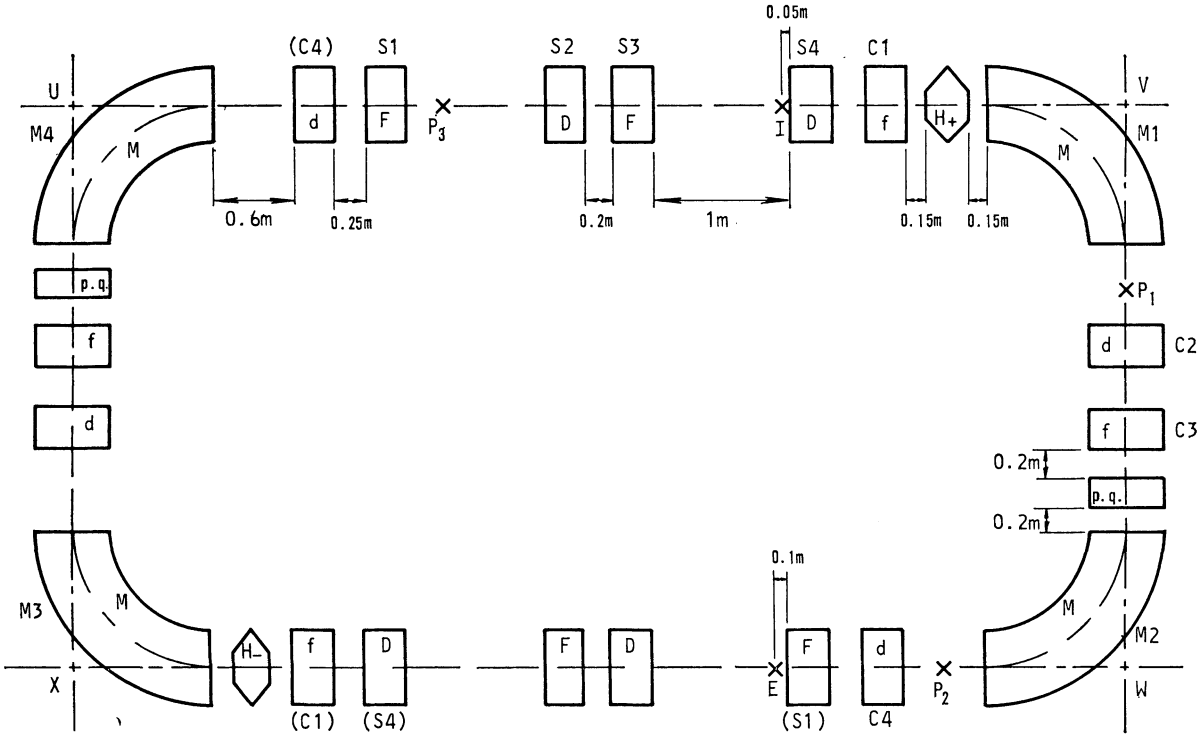

FIG. 1. Schematic of storage ring with identification codes for quadrupoles and magnets, and bench marks, U, V, W, X used for alignment. For component dimensions and details see Appendix I.

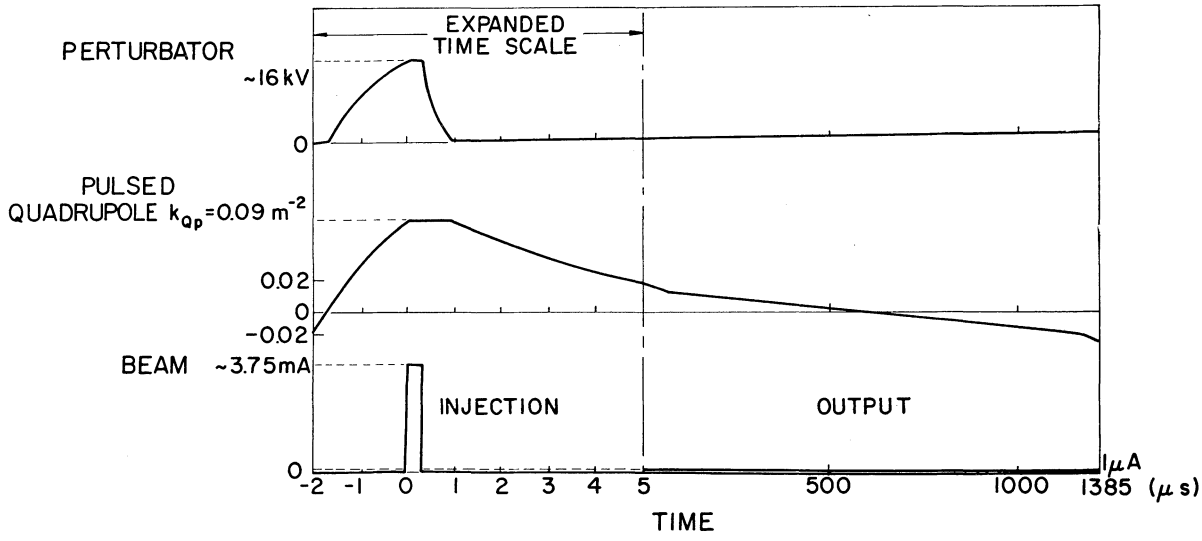

FIG. 2. Mode of operation of ring (Schematic). Note compression of abscissa scale for $t > 5$ μsec.

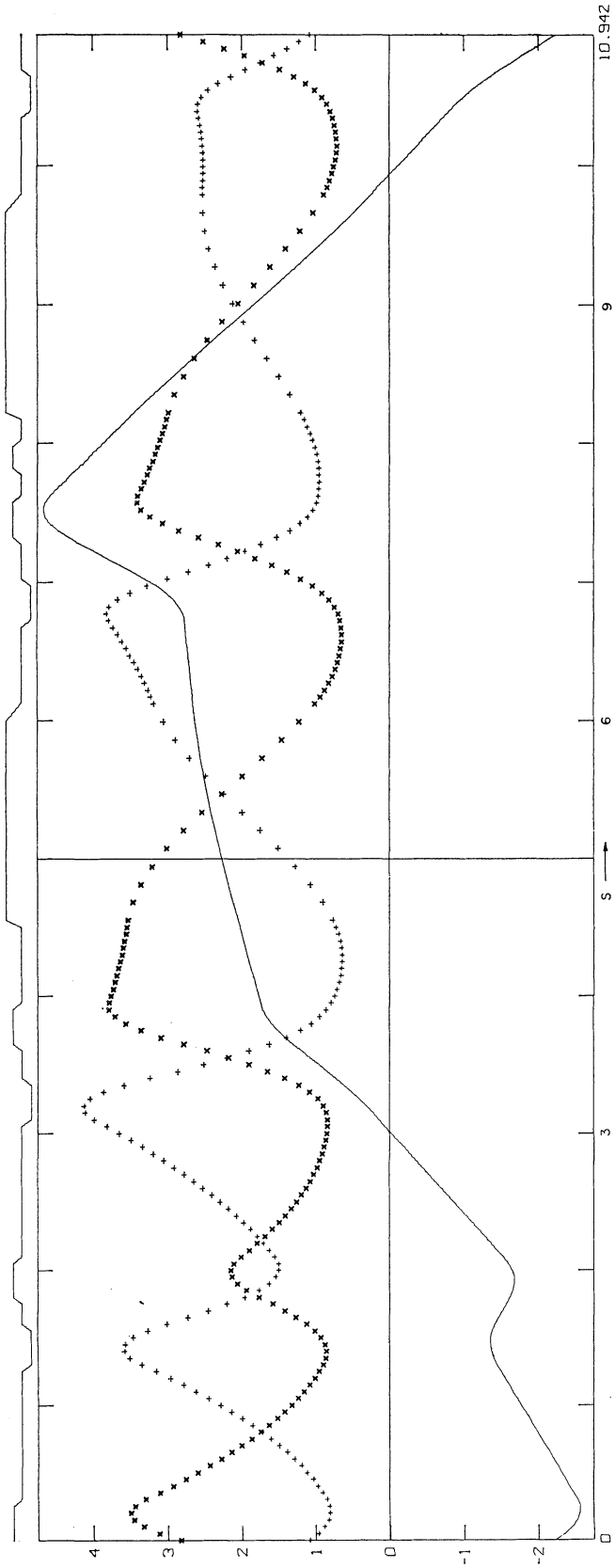

FIG. 3. Betatron β and g functions (β_x shown by $\times$, β_z by $+$, g by solid line). All scales are in metres, but, since g is dimensionless, we plot as solid line Rg in m (this scale can also be read as mm displacement for $\Delta p/p = 0.1\%$). Origin is at the end of the 25-cm drift section which is dimensioned in Fig. 1, curves extending over *half* the ring. The line above the graph on this figure indicates the positions of the ring components, which begin or end at the right-hand end of the sloping portions. A central position (vertically) indicates a drift space, smaller upward (+) or downward (−) displacements are for quadrupoles (F and D respectively), and a larger upward displacement is for bending magnets.

TABLE I
Alternative ring designs

Ring	(1)	(2)	(3)	(4)	
SPECIFICATIONS:					(units)
$\Delta E/E$, energy band accepted	0.1	0.1	0.15	0.15	%
Beam emittance (x-plane)	8	4	4	4	mm-mrad
(z-plane)	8	5	5	5	mm-mrad
Spot drift (additional)	no	no	no	± 0.5 (x and z)	mm
Injection orbit shift	15	12	12	12	mm
DERIVED QUANTITIES:					
Position of ejection septum (x)	30.5	27	28.5	30	mm
Position of injected beam (x_b)	6.7	5.7	5.85	6.20	mm
Slope of injected beam (z'_b)	9.852	7.97	9.00	9.00	mrad
Position of injection septum (x_c)	0.2	0.2	0.35	0.7	mm
Pulsed quadrupole (p.q.) strengths					
at start (+)	21.95	16.15	17.85	27.35	m^{-2}
at start (−)	19.35	16.15	19.4	27.3	m^{-2}
at end (+)	−16.2	−14.25	−10.75	−12.25	m^{-2}
at end (−)	−21.65	−18.25	−18.35	−19.0	m^{-2}
Max. beam envelope (x)	84	74½	84¼	92¾	mm
% $\Delta\nu_x$(of $(\Delta\nu_x)_e$) achromatic	81½	88½	76	85½	%

NOTES: For *p.q.* strengths, start/end refer to injection period; (+), (−) to limits of ΔE, energy range stored.
For x_b, x_c etc., see Fig. 13(b)—for other quantities, including dx_b/ds and z_b, see Table A-I. Note: we write z'_b for dz_b/ds.
$\%\Delta\nu$ refers to fraction of extraction working range ($(\Delta\nu_x)_e$) during which whole ΔE range of energies is being ejected

motion) is to 2⅓, the smaller the triangle; reducing ν_x slowly from a value near 2.343 towards 2.333 causes the gradual ejection of all the beam. The areas of both the injected beam (in x-phase-space) and of the stability triangle (S_Δ) depend on energy. In Figs. 5–8 the pulsed quadrupole strength is shown as a parameter at the right of the family of curves giving the variation for S_Δ. These curves show how these variations, for $\beta = 0.475$, can give rise to a substantially achromatic extracted beam—as the ejection proceeds, the change in pulsed-quadrupole strengths causes the 'sweeping-out' of the occupied area ABCD of these figures. For other values of β, as for example in the curves of Figs. 6(a) and 6(b) of Ref. 1, the slopes of the 'sweeping' lines differ appreciably from those of AB or DC on the same figures, so that ejection occurs at different times for different energies. For example for $\beta = 0$ the fraction of the whole ejection period during which all energies (within the ΔE) are being simultaneously extracted, may fall to about 15% (cf. Fig. 6(a) of Ref. 1), based on a linear pulsed-quadrupole variation with time. Even if an optimum nonlinear pulsed-quadrupole variation is arranged this figure may still only be about 25–30 %.

Table II lists the principal parameters which result for the four alternative designs proposed; part (b) of this table, concerning the 'step' attainable at extraction, will be discussed in Sec. 7 below.

3. SUMMARY OF EFFECTS OF POSSIBLE DEFECTS IN THESE RINGS

A separate report[6] presents a detailed study of many defects which affect the performance of a ring, including possible mechanical misalignments as well as questions of the accuracy needed in the fields in the ring components. Because of the detailed nature of these studies, only the results are given here; the methods employed follow closely those of prior studies of similar systems.[9,10]

Apart from the difficulty in this type of study of distinguishing 'systematic' from 'random' errors of positioning or designing elements, there are problems of how the effects of different possible defects or misalignments may combine. The various defects, which include displacements, tilts, twists (cf. Fig. 4(c) for coordinates used), field-strength and field-gradient errors, as well as nonlinear field laws or harmonic content of a quadrupole field,

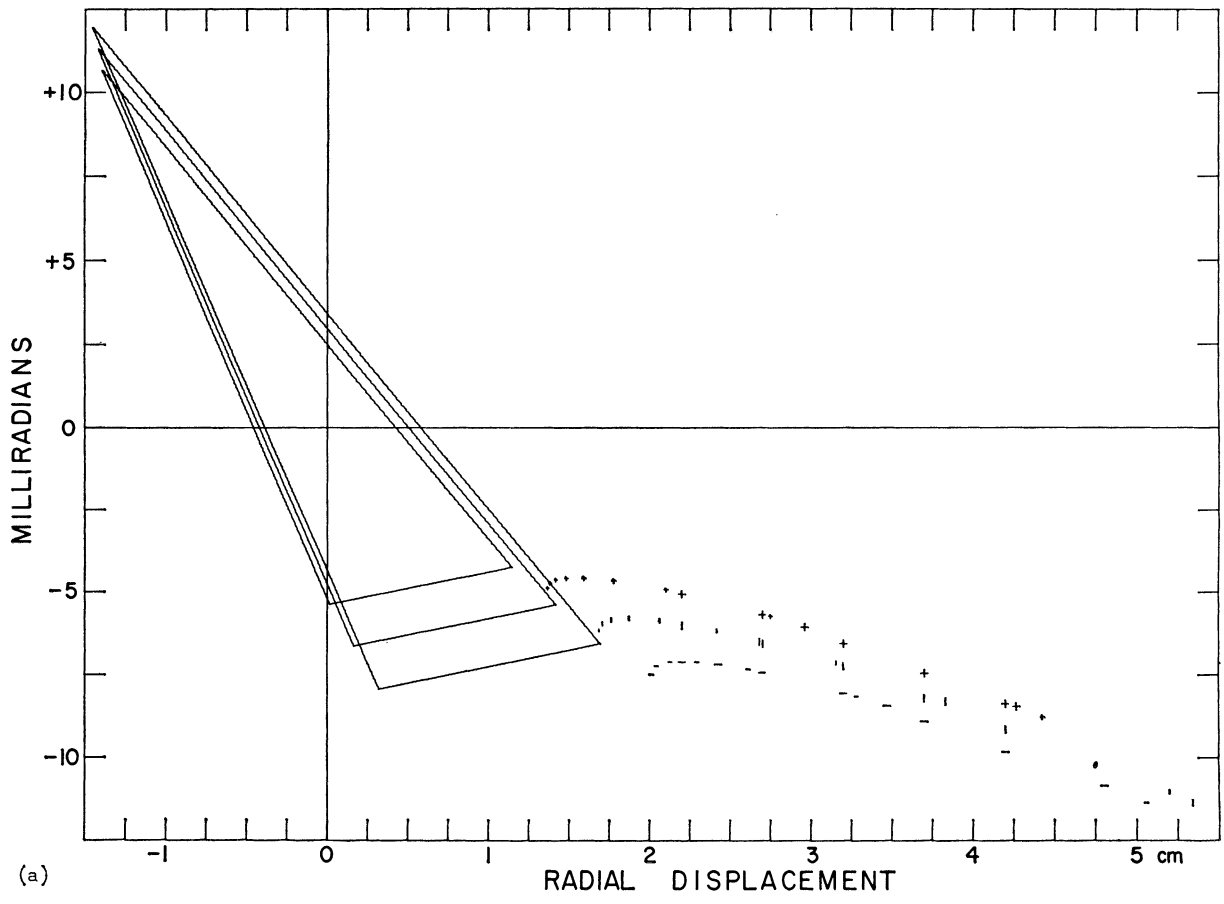

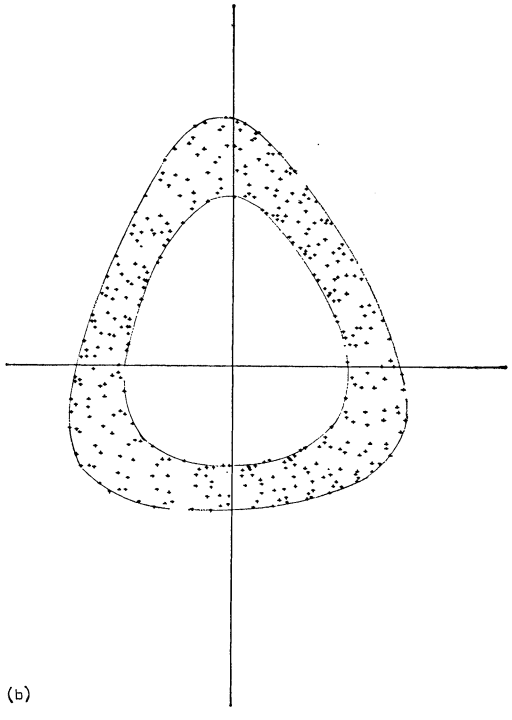

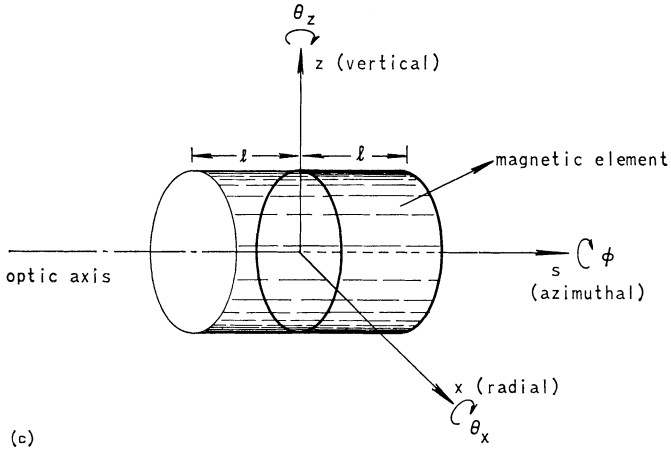

FIG. 4. (a) x-phase-space stability triangles and points showing trend of asymptotes (starting positions arbitrary); (b) x-phase plane diagram for injected beam; (c) System of axes used for misalignments (cf. Appendix II).

may produce effects of three kinds: they alter the ring tuning (ν_x,ν_z), the closed-orbit† location (x_{co},z_{co}) or cause dilatation of the beam envelope ($\Delta x_{env},\Delta z_{env}$). In Appendix II these are discussed with other relevant remarks on notation, e.g. the distinction between limits of error and root mean square values, and the terms 'tolerance' as distinct from 'required precision'. In our case the latter applies only where the effect is one on ν_x, whose precision is definable in terms of the duty-factor of the emergent beam for which the design is chosen, and other known ring properties; in other cases, mainly misalignments, the tolerances we use are postulated ones, whose computed effects appear to be acceptable, and which are similar to the tolerances assumed for other prior proposals.[3,4] Their values (Table A-II) also appear fairly easy to attain in practice. Slightly different values initially assumed in Ref. 6 for a few of these quantities were finally changed to the values given here.

The computed uncertainties resulting from these factors are given, as closed orbit shifts or envelope dilatation, in Table III. The values are for the first ring design, but only a few values are appreciably reduced (as indicated by footnotes) for the second ring; this occurs mainly where values are sensitive to the maximum displacement from the nominal orbit, e.g. in the extraction stage, or due to the larger injection amplitude used in the first ring. For the quantities described as "random" in this table, an $\sim 13\%$ increase has been applied where indicated, so as to yield 95% confidence limits, as explained in Ref. 6, even though their real precision may not justify the distinction. However, it is felt that the values of Table III should provide a reasonably safe guide to how much extra space is needed to allow for imperfections in the ring. Both arithmetic sums and root-mean-square (i.e. quad-

† The 'closed orbit' concept is basic to a ring device, being the orbit which exactly closes on itself (for ν_z and ν_x non-integral, it must be the condition of no betatron oscillations). However, for a nonideal ring it may be sinuous and cross and recross the ideal closed orbit position. The stability triangle apices represent special cases of closed orbits for an amplitude of oscillation yielding exact $\nu_x = n/3$ resonance, and these orbits close (at least in respect of x-plane motion) on themselves after *three* turns, not *one* turn.

TABLE II
Characteristics deduced for alternative designs

Quantity	Unit	Outer area		Hollow area		In exit channel	
(a) Phase-plane areas							
'N' Alternatives:		(1)	(2)	(1)	(2)	(1)	(2)
x-areas	mm-mrad						
$\Delta E/E = -0.05\%$		282	195	109.5	89.4		
E nominal		249	171.5	99.	78.8	45	~34
$\Delta E/E = +0.05\%$		229.5	151.5	90.	71.8		
z-plane areas	mm-mrad	~59	~29	~0	~0	~70	32–36
'W' Alternatives:		(3)	(4)	(3)	(4)	(3)	(4)
x-areas	mm-mrad						
$\Delta E/E = +0.075\%$		147	177.5	73.2	69.9		
E nominal		182	207.5	87.8	81.2	51	~65
$\Delta E/E = -0.075\%$		220	251.5	98.4	96.5		
z-plane areas	mm-mrad	~30		~0		32–36	
(b) Step values	Position of septum (x) mm	Start (−) mm		End (−) mm	Start (+) mm	End (+) mm	
Alternative (1)	31.0	4.85		13.3	10.4	19.2	
(2)	27.0	5.22		11.6	11.3	18.0	
(3)	28.5	4.93		12.3	15.5	22.7	
(4)	30.0	5.21		15.1	15.9	26.5	

The exit beam emittances given in the last two columns of (a) above are overall values.
NOTE: 'N' ('narrow') alternatives have $\Delta E/E = 0.1\%$, 'W' ('wide') have $\Delta E/E = 0.15\%$.

TABLE III
Summary of effects of misalignments or other errors (from Ref. 6)—for postulated tolerances of Table A-II

Effects (all in mm)	Δx			Δz		
	Closed orbit shift	Envelope dilatation	Notes	Closed orbit shift	Envelope dilatation	Notes
A. Systematic for elements concerned						
Magnet displacement δx, δs, δz	0.23_3		mx	0.65		mx
at septa—note (i)	small		inj	0.11		ej
Magnet index δn, angle of polefaces		0.10_5*	mx			
at septa, approx.		0.06*	mx			
Quadrupole strengths		0.06	mx			
Bending magnet half-length	0.50		mx			
~0 at inj; also	0.28		ej			
Bending magnet field	0.46_7		mx			
B. 'Random' (for different elements; × 1.13 to give 95%-confidence						
Quadrupole misalignment, tilt	0.99		mx	2.67		mx
at septa—note (i)	0.41		inj	1.05		ej
Quadrupole twist	<0.1	0.40**	mx	<0.1	0.30**	pre
at ej septum	~0.1	~0.1	ej	<0.1	1.36*	ej
Quadrupole longitudinal position		0.27*	mx		<0.1	mx
Magnet displacement or tilts	0.43		mx	1.01		mx
at septa—note (i)	0.18		inj	0.37		ej
Magnet longitudinal errors	~0.33		(included in previous item)			mx
Bending magnet twist				0.88		mx
at septa—note (i)				0.36		inj
Magnet index (n) error		0.44*	mx		trivial	
Quadrupole strength error		0.20*	mx			
Bending magnet half-lengths	0.46		mx			
~0 at inj septum; also	0.24		ej			
Bending magnet fields	0.58		mx			
~0 at inj septum; also	0.32		ej			
C. Arithmetic sums						
Systematic only	1.20	0.16	mx	0.65	—	mx
Random only	2.46	1.31	mx	4.52	1.35	ej
Total	~3.6	~1.5	mx	~5.2	0.30	pre
D. Quadrature sums						
Systematic only	0.73	0.12	mx	0.65	—	mx
Random only	1.31	0.68	mx	3.00	1.35	ej
Total	~1.50	~0.68	mx	~3.1	0.30	pre

NOTES: mx = at maximum value, ej = at ejection septum, inj = at injection septum, pre = prior to ejection stage

Note (i) Value at septum *not* given is near to value for 'mx'. Values are all for first alternative ring; if sensibly different for second ring, asterisks added (* = ~ 12½ to 15% less, ** = 20–25 % less). Generally the maximum values of different effects do not all occur at the same azimuth, so the composite results 'C' and 'D' above are likely to be pessimistic.
The overall total effects are therefore approximately (at worst): ±4 mm in x, ±5½ mm in z.
On quite reasonable assumptions (using quadrature compounding law) they would be expected to be of the order of half these values.

rature) addition values are presented, since the former almost certainly represent an over-stringent interpretation of the likely effects.

4. SUMMARY OF STABILITY OF FIELD STRENGTHS REQUIRED

The conclusions of Ref. 6, on the required stability for field strengths during operation, are less easy to summarize. In general, the required accuracies for initial settings of fields seem to be of the order of 1 part in 1500 in the quadrupoles and 1 part in 5000 in the bending magnets; it would be advantageous if both these settings could be made more accurately but the values quoted appear adequate. Since the field gradients are smaller in the bending magnets, maintenance of the tighter tolerance in these may give rise to no

more difficulty than the 1 in 1500 for the magnetic quadrupoles, which may be the more difficult to monitor. However, one particular combination of the quantities† involved sets the value of ν_x; the precision to which this must be held is definitely higher than would result from the accuracies quoted above. Also, ν_x is varied over the "working" range by means of the pulsed quadrupoles—if these are suitably biased, a small error in the ν_x value can be readily corrected. The reasons for this high precision in ν_x are that ejection depends on the exact difference $\nu_x - \nu_r$, where the resonant ν_r is defined as $2\frac{1}{3}$; if we set up the ring for 90% duty factor, the tolerance on the time at which extraction must begin must be only ± 1–2 % of the extraction period. In that period, the total ν-shift $(\Delta\nu_x)_e$ is only about 3.5×10^{-3}. Therefore the accuracy of setting ν_x is about $\pm 5 \times 10^{-5}$, corresponding to an accuracy of the strength of the

† ν_x depends primarily on the strength of the focusing quadrupoles (the defocusing ones mainly affect ν_z, whose tolerance is less stringent), and to a smaller extent on the bending magnet fields.

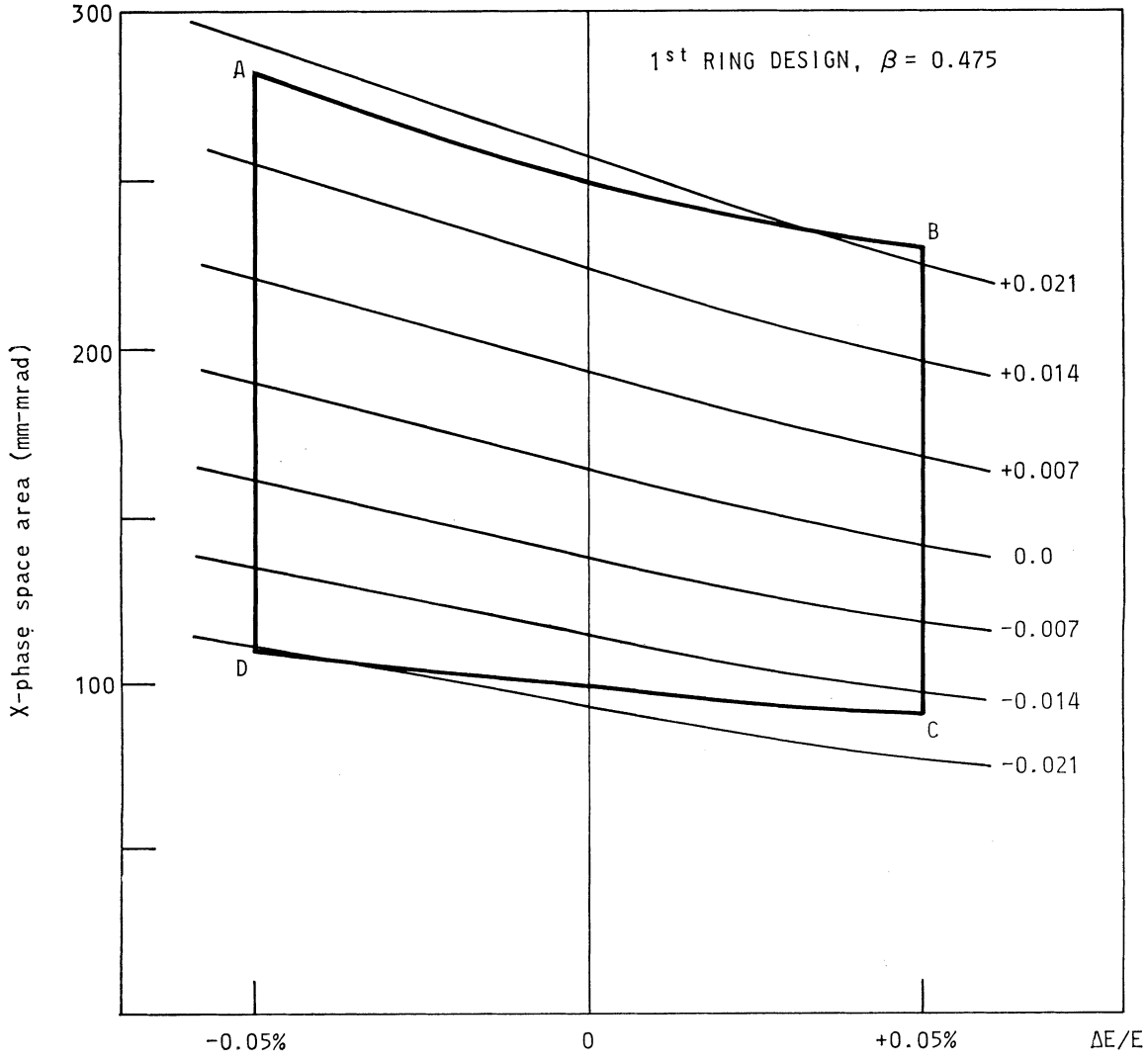

FIG. 5. Stability triangle x-phase-space area, pulsed quadrupole strength (in m^{-2}) as a parameter, also AB (start) and DC (end) for limits of ejection as a function of energy, $\beta = 0.475$, first ring design. Area ABCD is 'populated' region.

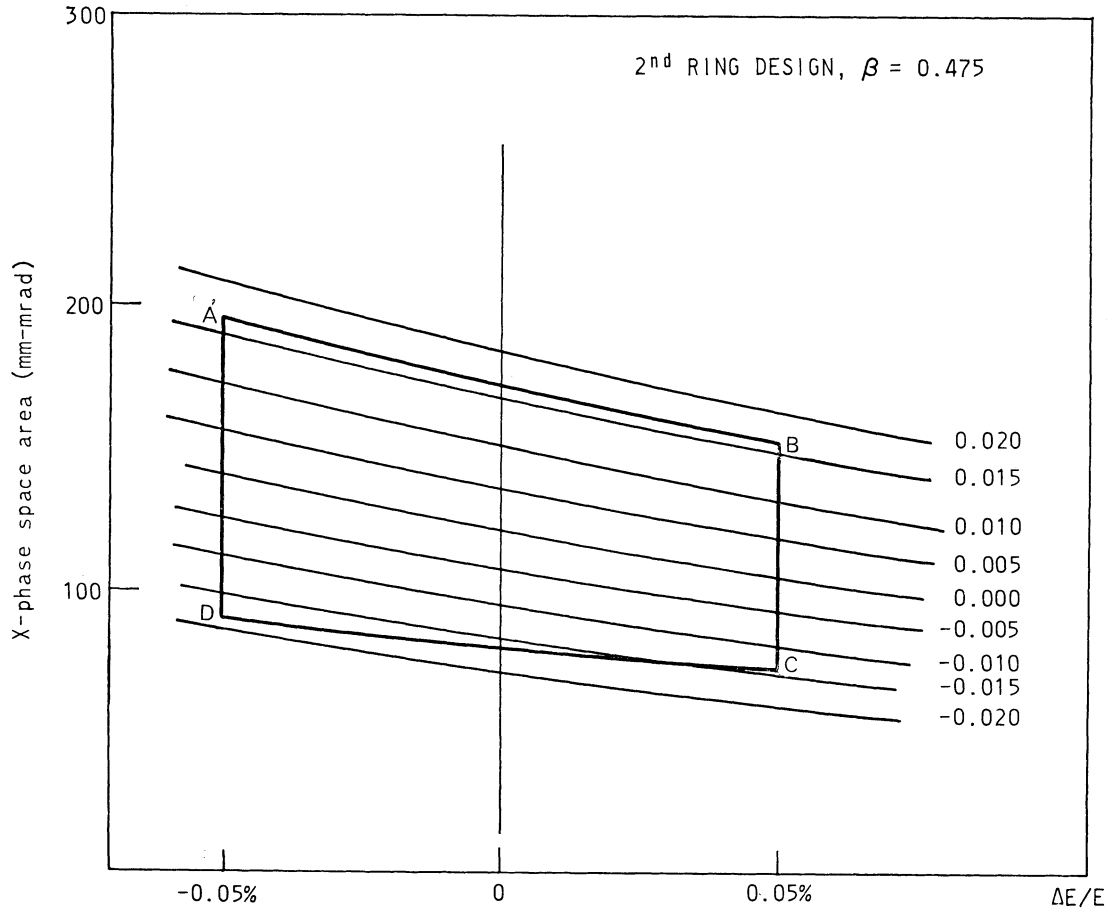

FIG. 6. Stability triangle x-phase-space area, pulsed quadrupole strength (in m^{-2}) as a parameter, also AB (start) and DC (end) for limits of ejection as a function of energy, $\beta = 0.475$, second ring design. Area ABCD is 'populated' region.

F and f quadrupoles† $\pm 2 \times 10^{-5}$ (in Ref. 6, where $\pm 1\%$ of $(\Delta\nu_x)_e$ was postulated, this result was given as 1 part in 75,000 for the most stringent case). However, if in practice it proves difficult to attain 1 in 40,000–60,000 in stability for a high-gradient magnetic field, and if it is acceptable to reduce the duty factor to 60–75 %, the tolerance on the time of onset of ejection rises to 15–30 % of the actual ejection period (or of $(\Delta\nu_x)_e$); the required quadrupole field accuracy then falls by a factor of 10 to 20, to around 1 in 2500, which seems quite feasible. Alternatively, at say 80% duty factor, the time of onset of extraction could be continuously monitored and used to drive a servo system controlling a bias on the pulsed quadrupoles, to correct for any drifts. It is thus admitted that in the commissioning of the ring a setting-up procedure of some complexity may be needed, and to a lesser extent also whenever the working energy of the ring is to be changed. Probably initially one would use an increased pulsed-quadrupole amplitude of variation; then by observing the time of onset of ejection, and how this varies with particle energy (within the ΔE range), settings can be chosen to give good operation with the normal pulsed-quadrupole waveform applied.

† Notation as in Fig. 1; we assume the fields in these four quadrupoles are correlated, e.g. as if all were energized in series.

5. SPACE CHARGE AND INSTABILITY EFFECTS

Two other results from Ref. 6 are relevant here.

The space charge limit for the ring current and the transverse resistive instability have been studied, as representing the factors most likely to limit the charge which can be stored in the ring. Assuming a pulse recurrence rate of 720 sec^{-1}, an injected current (for five turns, i.e. 365 nsec) not exceeding about 15 mA, corresponding to a "smoothed" output current of about 4 μA, should be quite safe if a stainless-steel vacuum vessel is used; if copper were substituted for stainless steel a larger current in the range of 60–100 mA injected, should be possible. In general, due to the $\Delta E/E$ restriction, these currents will be considerably lower than that of the original (unanalysed) linac beam, which may perhaps attain 0.25–0.5 A. For the experiments envisaged an output current of 4 μA appears likely to be ample; in fact, for many of them, a fraction of 1 μA in a 'smoothed' beam of duty factor $\sim 75\%$ would appear to suffice.

6. EXTENSION OF THE ENERGY RANGE ACCEPTABLE FROM 0.1 TO 0.15%

The first two alternative designs were for $\Delta E/E = 0.1\%$ but in order to study whether a larger $\Delta E/E$ was allowable the rings (3) and (4) (see Table I), designed for $\Delta E/E = 0.15\%$, were computed—ring (3) used the same beam emittance specification as ring (2), while ring (4) differed in that an allowance was made for drift of the beam spot. This makes it roughly comparable to the ring (1) design of Table I with 0.15% instead of 0.1% $\Delta E/E$.

The main consequential difference between these

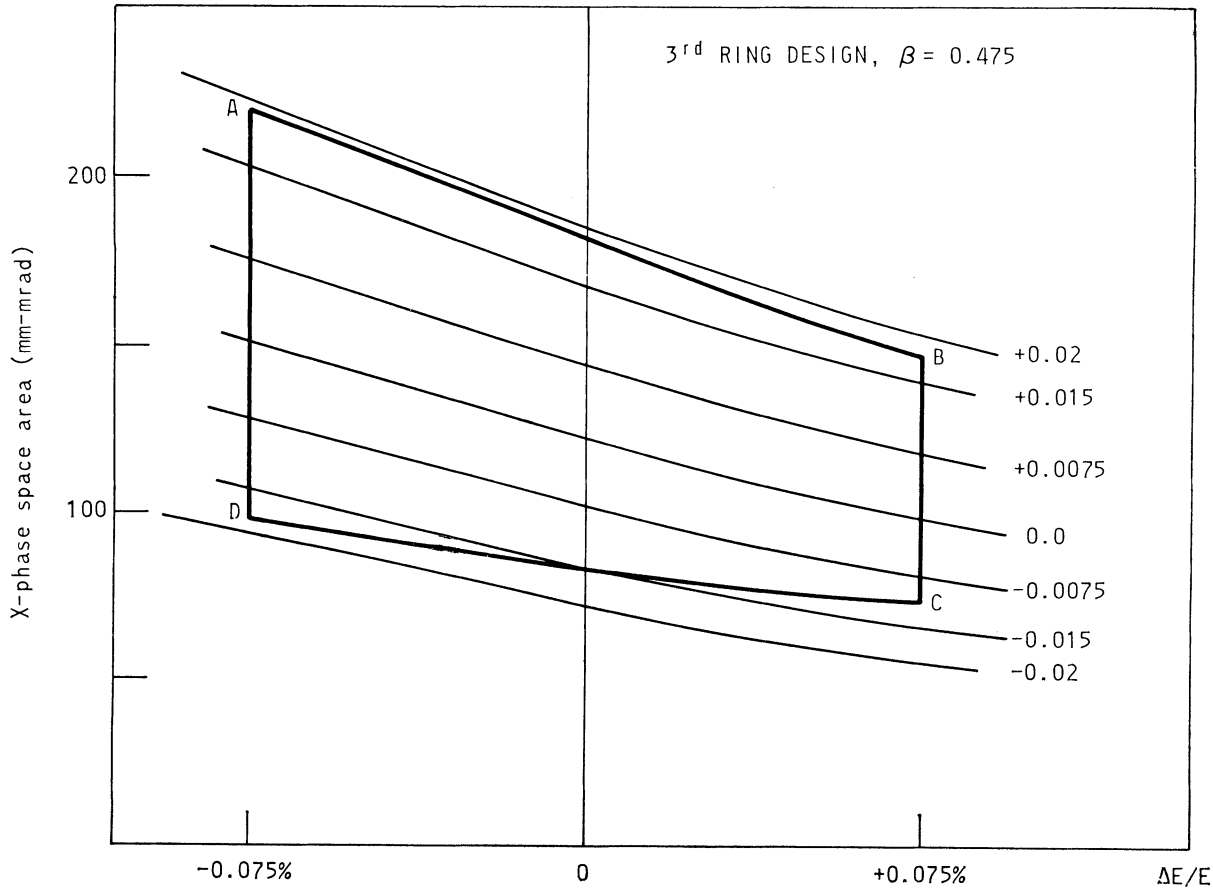

FIG. 7. Stability triangle x-phase-space area, pulsed quadrupole strength (in m^{-2}) as a parameter, also AB (start) and DC (end) for limits of ejection as a function of energy, $\beta = 0.475$, third ring design. Area ABCD is 'populated' region.

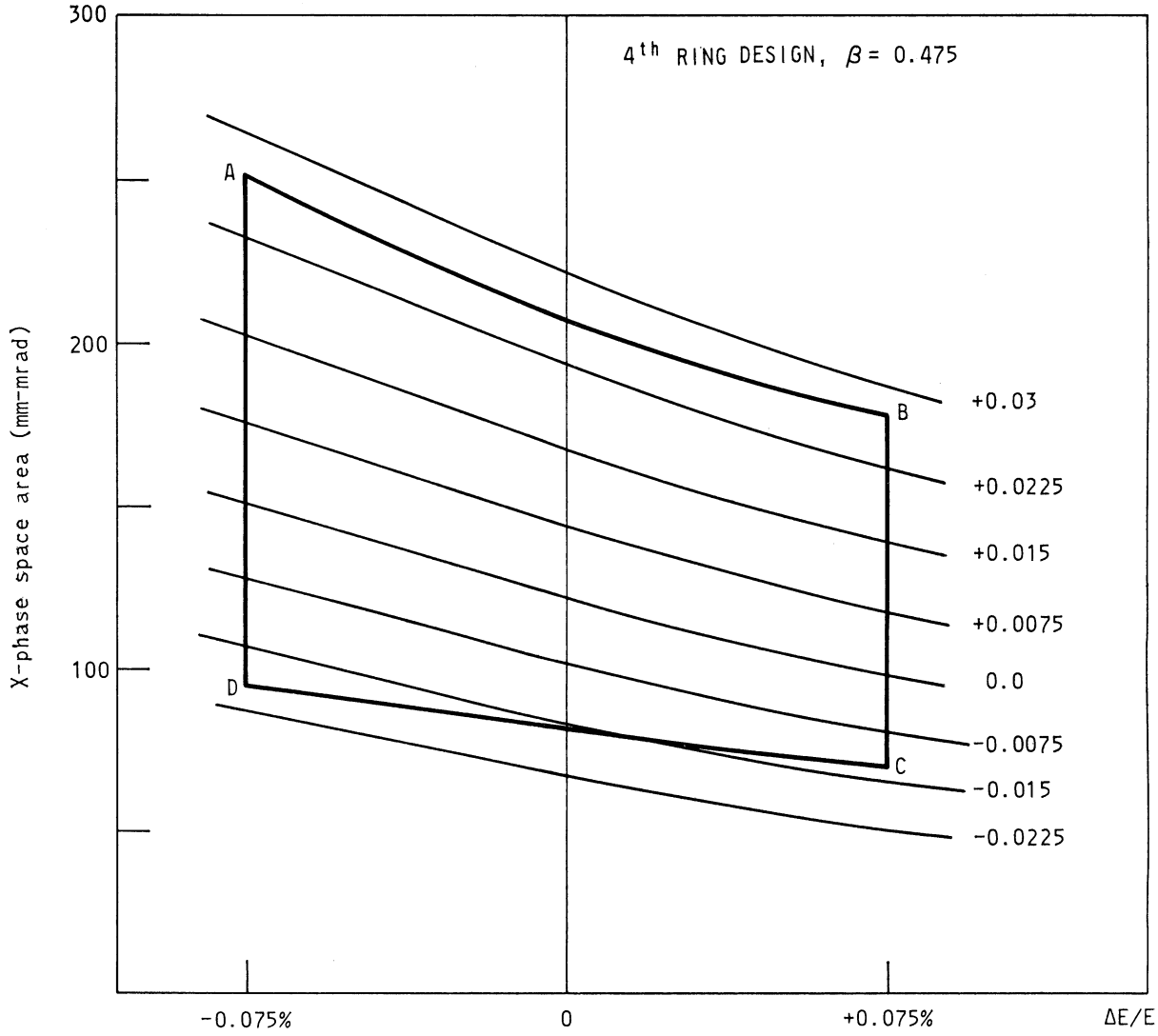

FIG. 8. Stability triangle x-phase-space area, pulsed quadrupole strength (in m^{-2}) as a parameter, also AB (start) and DC (end) for limits of ejection as a function of energy, $\beta = 0.475$, fourth ring design. Area ABCD is 'populated' region.

designs is in the apertures needed for the ring components, discussed in Sec. 7 below. The extraction conditions for these two alternatives are quite similar (see Figs. 7 and 8) to those for the first two rings, and for all of them $\beta = 0.475$ gives, to a good approximation, an achromatic extraction. The accuracy with which the S_Δ's for points ABCD on Figs. 5–8 is known is probably only about $\pm 3\%$, so that the small differences seen between these figures may not be significant. For example, ejection appears to start achromatically for ring (2), and at the end become nonachromatic over a period of $\sim 12\%$ of $(\Delta v_x)_e$; for ring (1) the end-of-ejection is similar but the start occurs somewhat earlier for positive $\Delta E/E$ compared with mid-energy or low-energy electrons (a condition which could be improved by increasing β slightly). For the wider $\Delta E/E$ or rings (3) and (4), we see that conditions are not appreciably worse. At the end of ejection the period of nonachromatic extraction rises to $\sim 18\%$ of $(\Delta_x)_e$ for both rings (3) and (4), although in fact at the start of ejection ring (4) has rather less variation with E than ring (1). For ring (1), an increase of β may improve

matters but for ring (3) the points B and C are within the pulsed-quadrupole range represented by A and D, so that for a limited range of values of β the achromaticity of the ejected beam would remain constant, giving an additional tolerance on the β-index of the bending magnets. These differences are therefore relatively trivial.

7. APERTURES REQUIRED FOR THE COMPONENTS OF THE RING

Since questions of cost and the availability of components may be crucial for any decision to build any ring of this type, the size of the required apertures for ring components, and hence the specification of the admittance of the ring, become of prime importance. As already explained, the linac beam emittances for rings (1) and (2) are alternative values which appear representative for the linacs which may be available. As stated above, the two values of beam emittance chosen as input data for rings (1) and (2) (see Ref. 5 and Table I) were values appropriate for the Toronto linac. We may note if the smaller of these values (5 mm-mrad vertically and 4 mm-mrad horizontally) were the actual beam emittance, at the injection septum, with the matching appropriate to the Twiss-matrix α's and β's at that point of the ring (see Table II), a ring admittance of 8 mm-mrad in both planes (as for ring (1)) would provide sufficient latitude for a beam-spot drift from nominal position of ± 0.66 mm vertically and ± 0.41 mm horizontally. In alternative 4 a more detailed set of calculations was made, for different spot positions (with the same 5 and 4 mm-mrad emittance), allowing for a spot drift tolerance of ± 0.5 mm in each plane, which corresponds to an overall specification closely comparable to that of ring (1).

Thus it appears that rings (2) and (3) represent a rather small but typical beam emittance with no (or with only a small) allowance for beam-spot drift, while rings (1) and (4) include an allowance (emittance increment) corresponding to about ± 0.5 mm drift. In practice some further reduction in emittance may still be possible, and in addition there is also the possibility of "scraping" the incoming beam, to reduce its drift or emittance or both, before injecting it into the ring. The loss of beam current which would result, and any additional background radiation, would have to be acceptable for the experimental system in question.

The other design parameters which determine the apertures needed are connected with the ejection process and include the 'pitch' or 'step' of the motion outwards in the x-plane in the last three orbits within the ring, for which values were given in part (b) of Table II. This quantity, which corresponds to the outward motion in the last three turns of an electron which just fails to hit the exit septum† in one orbit and then continues to move within the ring for three more orbits, is discussed further below. It seems to provide the main reason why $\Delta E/E$ should not exceed about 0.15% for the 'nonachromatic' design of ring we have adopted.

Interpreting the x-phase plane areas for the stable state by means of the β_x and β_z of Fig. 3, we find that the stable (i.e. before ejection begins) x-plane beam sizes are about ± 15 mm for rings (2) and (3), and somewhat larger, about ± 18 mm, for rings (1) and (4). In the z-plane the corresponding sizes are ± 4.2 or ± 5.5 mm, but here it must be remembered that during the five turns of injection, and (with a gradual decrease) for a few turns thereafter the beam in the injection region of the ring azimuth is displaced vertically by up to 15 mm (or 19 mm for ring 1). Adding reasonable tolerances, as indicated by Table III, this would lead us to expect to need x-apertures around 45–50 mm and a z-aperture of ± 20 mm (or for ring (1) near the injection septum a little larger value). In fact, it is relatively easy to accommodate the z-aperture; ± 2.5 cm everywhere (within the vacuum chamber) seems reasonable, so that, to allow space for alignment adjustments and the vacuum chamber wall thickness, a 6 cm vertical aperture between pole-tips is tentatively adopted.

For the x-plane, however, more space than indicated in the foregoing is needed to accommodate those electrons which have left the stability triangle but not yet reached the exit septum. Figs. 9 and 10 (for rings (1) and (2) respectively; ring (3) will be similar to (1) but ring (4) would give still larger values) show the actual envelopes which the limiting electron reaches during its last three

† On Fig. 4(a) the representative point is displaced outward close to the asymptote corresponding to its ΔE value, as indicated, for every three orbits executed in the ring.

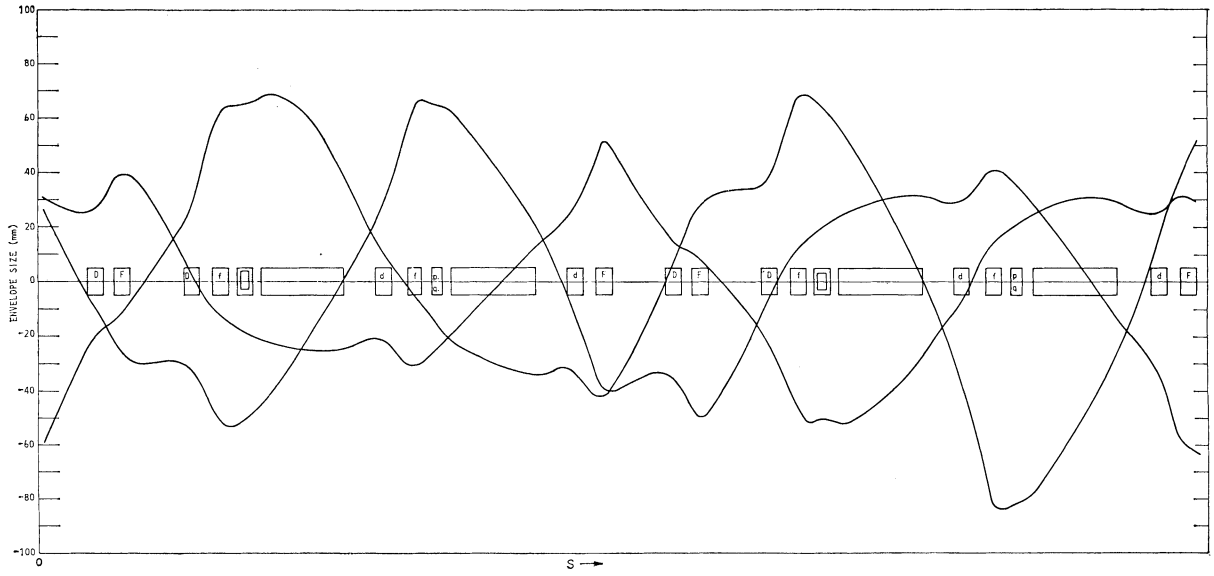

FIG. 9. Envelope of beam in x-plane in last three orbits, first ring design.

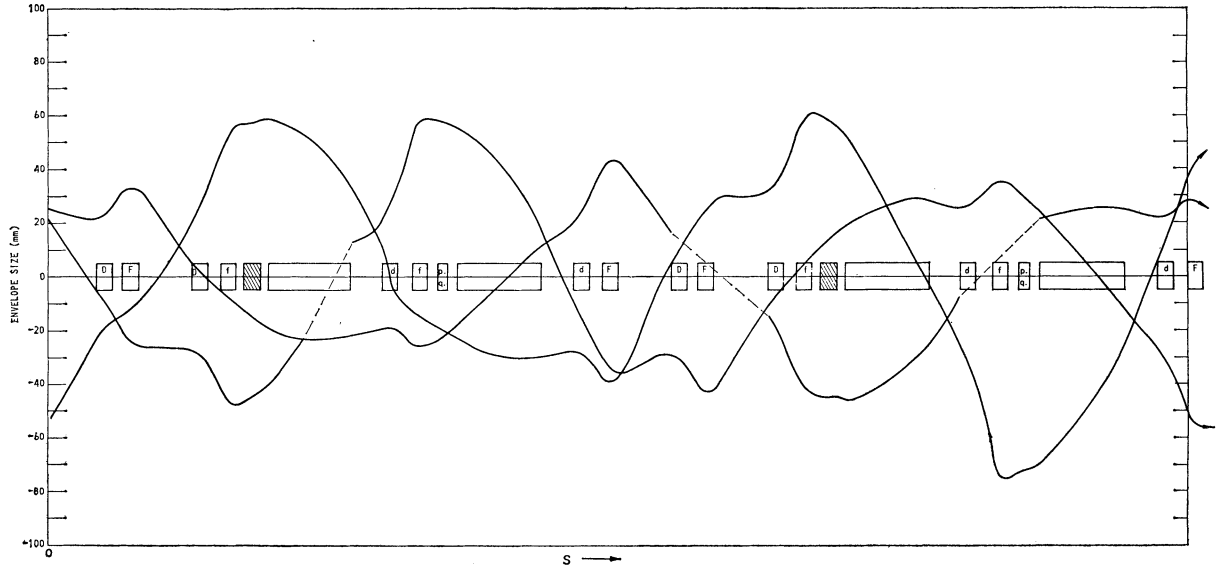

FIG. 10. Envelope of beam in x-plane in last three orbits, second ring design (dotted sections approximate).

orbits in the ring, neglecting effects of any misalignments. The maximum envelope excursions, as shown in Table III, for the four designs we use are respectively, 84, $74\frac{1}{2}$, $84\frac{1}{4}$ and $92\frac{3}{4}$ mm. Actual envelope limits, including misalignment effects, for rings (1) and (3) would therefore be about 87 mm, and for ring (4) $\sim$ 95–96 mm. It is true that these values occur in only one element (a quadrupole) of the ring,† and it may be possible to set the closed orbit so as to ensure that the misalignment tolerances reduce or leave unchanged, or at least do not greatly increase this excursion of the

† The pulsed quadrupole adjacent to the unit where the maximum x-amplitude occurs in fact requires the aperture only $\sim 5\%$ smaller, but this is a low-field unit and should not present any real difficulty.

limiting particle. Certainly this one quadrupole will need to have an aperture of at least 7 inches. In a later section this point is considered further.

However, one conclusion from these arguments is that a $\Delta E/E$ as large as 0.15% would only seem reasonable if the required admittance for the linac beam, including allowance for any beam-spot drift, corresponds to a ring admittance of 4 or 5 mm-mrad or less; even for this case a $\Delta E/E$ no greater than 0.12% would be preferable. This is due to the technical limitations of quadrupole manufacture and other similar practical questions, so that with further studies some revision of this conclusion may become possible.

8. FURTHER POINTS CONNECTED WITH EJECTION AND APERTURES NEEDED

With the one-third resonance extraction method performance can be optimized by a suitable choice of several parameters, such as the strength of sextupoles (and therefore the nonlinear terms), the distance of exit septum from the closed orbit and the radial width of the exit channel. The septum thickness (taken as 0.002 in.) must be much smaller than the smallest 'step' used; since the rate of radially outward motion is larger for larger radial displacements, a step of one hundred times the septum thickness still means that something approaching 2% (rather than the 1% predicted on a simple basis) of the electrons will strike the septum. The minimum 'step' for our designs is therefore taken to be 5 mm, which defines the sextupole strength necessary. It was found that to obtain this value, the septum position has to be at least 1.4 times as far in the positive direction as the nearest corner† of the stability triangle (Fig. 4). To minimize the aperture required, the only remaining disposable parameter is the radial width of the exit channel, which should in fact equal the largest 'step' for the limiting electron. The smallest steps correspond to opposite corners (A and C) of the rectangle ABCD in Figs. 5–8, and the steps (see Table III) at the other two corners are of intermediate size. It is found, for $\Delta E/E =$ 0.1%, that the largest steps can be kept near or below 20 mm, but for 0.15% it is necessary to allow steps up to 23–25 mm. This is a result of the basically nonachromatic character of our rings—when the lines AB or DC of Figs. 5–8 lengthen due to the 50% increase in $\Delta E/E$, the step-size variation increases and so renders the aperture requirement difficult to meet. Even for a monochromatic ring the step would vary by a factor of about two from start to end of ejection. The aperture required at the point in the ring where the envelope is numerically largest is at least 50% larger than at the ejection septum, as is seen from Figs. 9–10, the largest (inward) electron displacement occurring for our rings five units back along the last orbit from this septum.

The emittance of the extracted beam also varies with energy. Both its width at the septum (5 mm for $\Delta E/E$ at its negative limit at the start of ejection changing to ~ 20 mm or more for $\Delta E/E$ positive at end of ejection) as well as the angular divergence of the beam change. Figure 11 illustrates this effect; for more detail reference 6 should be consulted. The total area of these rectangles is the quantity given in the 'exit channel' columns of Table III.

These large excursions from the closed orbit, and the associated need to use at least 7 inch bore quadrupoles raise technical problems as well as increasing costs; these are briefly discussed in Appendix III and more fully in Ref. 6. The ease of obtaining large-aperture relatively short quadrupoles with satisfactorily harmonic-free magnetic fields may in fact determine just how far the ring designs can be pushed. Two design modifications appear to merit further study in view of these practical limits; one of these may be helpful in all cases while the other is mainly applicable if $\Delta E/E > 0.1\%$. To take the latter first, and realizing that the 'step' size is rather large for $\Delta E/E \sim$ 0.15%, it may be worth examining whether reducing the sextupole strength to 5 or 5.5 m^{-3} would give improved characteristics. This argument may be specially cogent for the larger admittance case (ring (4)), where a beam spot drift allowance was included). In fact, it was consequent on the generally scaled-down displacements which occur in going from the design of ring (1) to ring (2), that the sextupole strengths were increased from $\pm 5\ m^{-3}$ to $\pm 6\ m^{-3}$. Since these are the

† As an example, for ring 2, the stability triangle apex with the largest positive x coordinate is at $x = 20.6$ mm (compared with $x = 28$ mm for the septum), although by the time ejection ends, the largest x apex position falls in the range $8 < x < 14$ mm, depending on E.

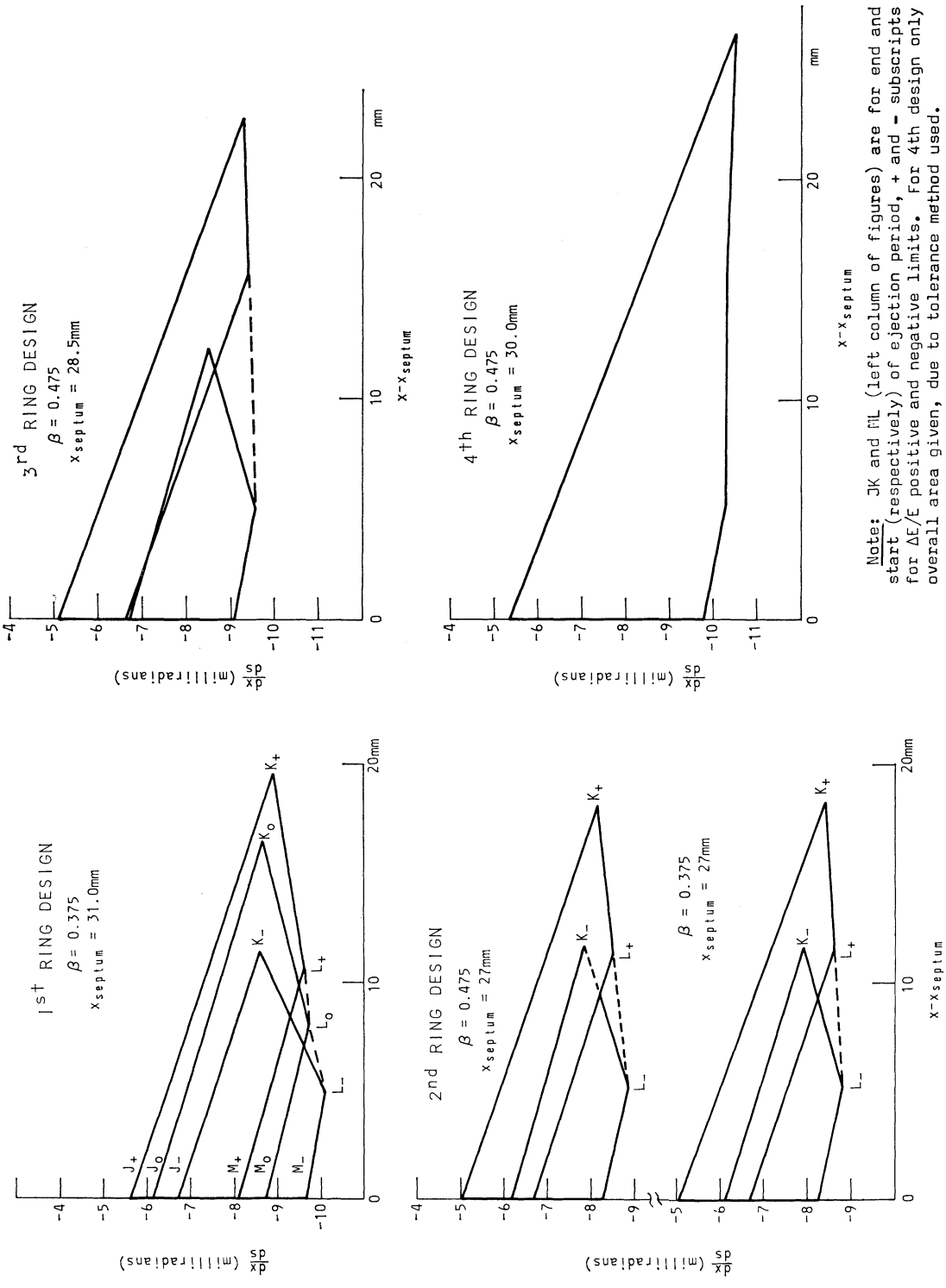

FIG. 11. x-phase-plane diagrams for beam at exit septum, for alternative designs (compare Tables I, II). For 1st design $\beta = 0.375$ version given, while for 2nd design diagrams for both β's are given to show that the changes which occur are trivial.

components of the ring which give rise to the nonlinear terms, a greater strength combined with smaller displacements should result in comparable effects due to the nonlinearities, as mentioned in Appendix I. But when, in changing from ring (3) to ring (4), the beam size was again increased, it might have been logical to revert to the 15 mm orbit perturbation† and to reduce the sextupole strengths to $\pm 5\,m^{-3}$. One should therefore examine, if a large-admittance $\Delta E/E > 0.1\%$ design is desired, whether the change to $\pm 5\,m^{-3}$ sextupoles, either alone or in combination with larger strengths for the perturbators, would be advantageous.

The second point is more generally applicable and also easier to explain. The envelopes of Figs. 9–10 show only one (numerical) maximum, five units before the extraction septum, but in the other three *f* (curved section focusing) quadrupoles the envelope is also rather large; but in each of these it is smaller by a factor of very nearly 1.2 than in the 'worst' unit. In two of these units the maximum is also in the last orbit before ejection, but for the *f* quadrupole next to the other pulsed quadrupole (half way round the ring from the 'worst' unit) it occurs in the penultimate orbit. Since the principal harmonic component (the 10th harmonic) which causes the nonlinearity of the field at large x's has a relative strength proportional to x^8, this factor of 1.2 gives a reduction in harmonic effectiveness of about 4.3:1. If, in fact, the quadrupole defects are only some 2.5 or 3 times too large for satisfactory performance, it would appear that the solution may well be to make the one 'worst' unit 20% larger in all dimensions—length as well as aperture. Such a larger unit, otherwise similarly designed, would have only $\sim 23\%$ as much nonlinearity as the unit replaced; while the defects of the other three quadrupoles mentioned would then produce effects of similar magnitude, these would almost certainly cancel one another to some extent due to the relative phases of the betatron waves they produce in the orbit for the "worst" particle.

Such a design, using one 36 cm long (effective length) quadrupole of 8.4 inch aperture, has not yet been studied in detail but the inter-unit spacing appears adequate and the strength needed for this one quadrupole was found to be near $3.2077\,m^{-2}$.

Figure 12, referred to in Appendix III, is an approximate treatment of the effect, in the 'worst' quadrupole only, of a 1.5, 2.5 or 4% field defect for the limiting particle, and shows that the emittance of the extracted beam is not too severely affected by a $\sim 2\%$ defect, but that larger ones are undesirable. Whether or not these design modifications are needed, the fact that the fields required are all quite low—about 1250 G in the bending magnets and 400 to 600 G at the pole-tips of the quadrupoles—should simplify the design problems and result in relatively low costs. The largest quadrupole pole-tip fields are in the straight section, so that even an aperture increase to 8.4 in. as proposed for the 36 cm (effective) length special quadrupole, still only requires a pole-tip field of ~ 425 G in this unit. On the other hand, a field monitor of say 0.1 or 0.04% accuracy in so low a field may raise some problems in

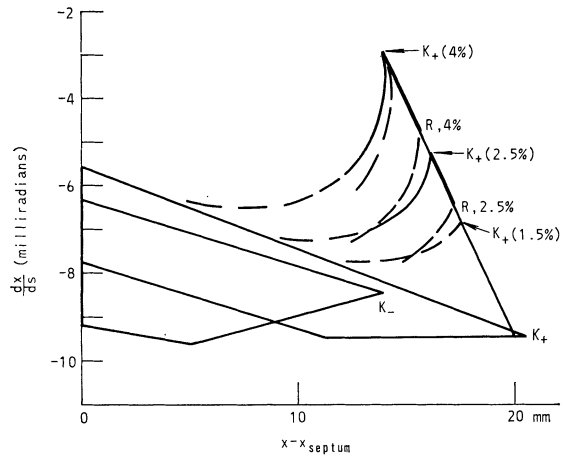

FIG. 12. Diagram similar to Fig. 11 for one case ($\beta = 0$, first ref. design) showing effect of quadrupole nonlinearity. Original K_+ corner has been truncated by a septum thickness allowance and its position for three magnitudes of defect is shown. At $4\frac{1}{2}°$ off x-axis (see text), the reduced displacement is indicated by R for 4% and 2.5% defects. Points on thicker lines between K_+ and R will tend to cluster near K_+. Dotted curves are approximate as indicated by calculations. Note: displacement of point K_- will be only about 32% of K_+ displacement (r^8 law).

† The change, cf. Fig. 13(b), of dimension x_w from 6.5 to 5.5 mm was also associated with the 15 mm orbit shift of ring 1; it is not clear whether this would be desirable for a revised ring 4 design.

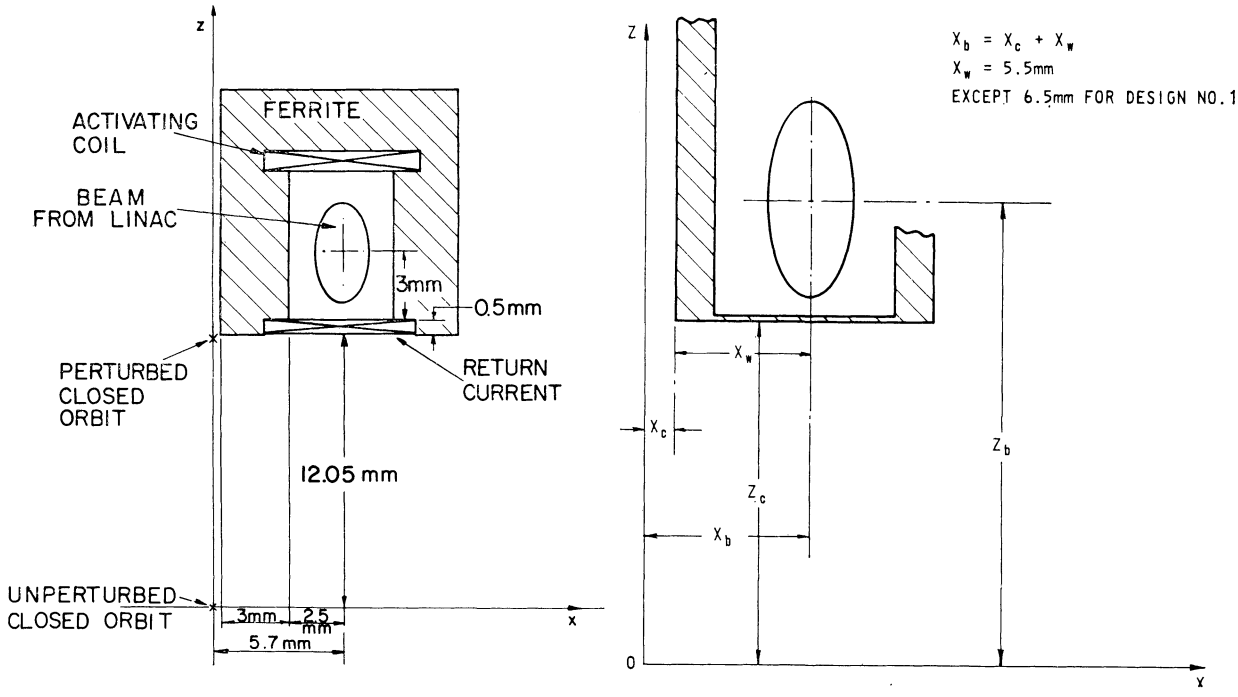

FIG. 13(a) Section at inner end of 2nd ring injection septum; (b) Scheme for dimensions for injection septa, for the alternative rings (cf. Tables I and A-I).

instrumentation, especially for the high gradients to be found in quadrupoles.

A few other points may require some care and either the fabrication of a prototype or some further theoretical study; an example is the injection septum of Fig. 13(a).† While no serious doubts are felt concerning the feasibility of a ring of this type, practical points such as beam spill and the resulting radiation damage or activation will need attention once the specification of the incoming beam available has been established, but no abnormal problems are foreseen.

The remaining questions are the design of beam transport systems from the linac to the storage ring and from the ring to an experimental set-up. For example, the magnets just outside (but close to) the ring, described as 'M_{en}' and 'M_{ex}' in Appendix I, form part of these beam transport systems, and must be magnetically shielded so as not to disturb the ring operation. Also two quadrupoles ($S2$ on the injection side and $S3$ on the ejection side) may have to be made specially to incorporate channels in their outer sections (for the entrance and exit channels). Studies of these beam transport problems have been deferred until a system layout and a satisfactory specification for beam locations are available.

† This figure is dimensioned for ring 2; for other alternatives the positions given in Table I and A-I using coordinate system of Fig. 13(b), would be substituted.

9. CONCLUSION

A set of four alternative designs, for two values of beam admittance and two of energy spread, for a storage ring for duty-cycle smoothing has been produced, and for the purposes indicated[2] the resulting designs would appear likely to be fully satisfactory. These are not inherently achromatic designs, but an output beam which contains all energy particles for most of the time is produced; however the different energies are distributed non-uniformly on an x-plane phase diagram, so that the subsequent beam transport system should be designed to pass the entire beam if the achromatism achieved is to be fully preserved. What is still needed is a full specification of the incoming beam from the linac, and of a desirable output duty factor and width of the band of energies to be stored (which should not be more than about

0.15%); the best approach to select a final design for a given set of specifications has been discussed. In particular, the duty factor can be raised at a later date if it is found possible to achieve a greater stability of field-strengths in the ring magnets and quadrupoles than is initially supposed, or if the somewhat conservative theoretical assumptions are found to be unnecessarily stringent. Further studies, e.g., on costs or of problems in particular components, may be needed but no major difficulties are foreseen.

ACKNOWLEDGEMENTS

The author wishes to acknowledge computing assistance from Dr. J. C. Kim, attached to AECL from the University of Toronto, with whose permission we quote results from Ref. 6. He is also indebted to Prof. R. Servranckx and Dr. J. L. Laclare for useful discussions and for making computer programmes available for this work.

REFERENCES

1. C. H. Westcott, *Proc. 8th Int. Conf. on High Energy Accelerators, CERN, Geneva, 1971*, p. 159.
2. J. W. Knowles, Atomic Energy of Canada Limited, unpublished internal report AECL CRNL-511.
3. R. A. Beck *et al.*, ALIS, an electron linac beam stretcher (project), presented by H. Bruck at *7th Int. Conf. on High Energy Accelerators, Yerevan, 1969*, Vol. II, p. 94.
   See also internal reports (series SOC-ALIS) especially SOC-ALIS-32 (1970).
4. R. Servranckx and J. L. Laclare, IEEE Trans. Nucl. Sci. **NS-18,** No. 3, 204 and 207 (1971) and papers cited there (SAL-RING series).
5. C. H. Westcott and J. L. Laclare, Atomic Energy of Canada Limited, unpublished internal report CRNL-542, Parts I and II.
6. C. H. Westcott and J. C. Kim, Atomic Energy of Canada Limited, unpublished internal report CRNL-542, Part III (in draft, to be issued).
7. H. Bruck, *Accélérateurs Circulaires de Particules* (Presses Univer. de France, 1966).
8. J. J. Livingood, *Optics of Dipole Magnets* (New York Academic Press, 1969) esp. chapter 18.
9. J. L. Laclare, Saskatchewan Accelerator Laboratory Report SAL-RING-20.
10. G. Gendreau, Saclay report SOC/ALIS-19.
11. W. C. Elmore and Garrett, Rev. Sci. Instr. **25,** 480 (1954). These authors give B_r but B_z is readily obtained from Eq. (4) by differentiation; we also take $\phi_n \approx 0$ or $\approx \pi$ for symmetry reasons. For more detail see also Cobb *et al.*, IEEE Trans. Nucl. Sci. **NS-12,** No. 3, 395 (1965) and SLAC 1965 Magnet Symposium, p. 431. 1965.
12. J. L. Laclare, OSECO: Second order beam transport programme (also in thesis, Orsay, France, no date) Saclay report SOC 69.3, July 1969.

Received 2 January 1973
and in final form 27 March 1973

APPENDIX I

General Form and Constants of the Storage Ring Designs

This appendix, together with Fig. 1, gives the schematic layout and information on the dimensions of the ring and of its components, sizes shown being 'effective lengths' including fringe field effects. Tables I and II (in the main text) give the main parameters for each alternative design while Table A-I gives those constants which are the same for all of the four alternatives, or for three of them, with the fourth different.

The units shown in Fig. 1, and their effective lengths, are as follows:

M. Bending magnets, 90°, 1-m radius (lengths $\pi/2$ m), $n = 0.5$; $\beta = 0.475$.

D,F,d,f. Fixed-field magnetic quadrupoles, 30 cm long

H_+,H_-. Sextupoles, of opposite polarity, 30 cm long

p.q. Pulsed (electrostatic) quadrupoles (see Fig. 2 for field variation with time) 20 cm long.

I,E are the positions of injection/ejection septa (these components lie to the left of the points shown, which are the effective septa locations).

U,V,W,X, are 'bench-marks' used in aligning the ring components; they form a horizontal rectangle of exactly 4.1 × 7.7 m size.

P_1,P_2,P_3 are vertical electrostatic deflectors (perturbators). Since these are specified by milliradian deflections, only their centre-points are indicated; their lengths can be chosen later. For time-variation waveforms see Fig. 2.

The length of the injection and ejection septa (probably about 50 cm) and the fields needed will be defined when the site of the ring has been chosen. Also, the entrance and exit channel magnets (M_{en}, M_{ex}) close to but outside the ring will be needed; these and the septa are similar to IMI, EMI, and IEI, EEI of Fig. 1 of Ref. 5. The

TABLE A-I
Quantities which are similar for all rings

Twiss-matrix values at injection	$\alpha_x = 0.0250_5$,	$\beta_x = 0.8377$ m
Curved section quadrupole strengths (in m^{-2}) d = -3.6393_5,		f = 3.8525_5
Injection value of pulsed quadrupole strength $+0.09\ m^{-2}$		
Effective lengths of D, F, d, f, H_+, H_- all 0.3 m; pulsed quadrupoles 0.2 m		

Quantities which differ for only one alternative ring

	Units	Values (for three)	Exceptional value	For Ring No.
Twiss-matrix values at injection, α_z	—	−1.6875	−1.679	1
Twiss-matrix values at injection, β_z	m	3.8893	3.859	1
Injected beam position, z_b	mm	15.405	18.912	1
Injected beam slope (dx_b/ds)	mrad	−0.20	−0.10	2
Injection tuning ν_x	—	2.35132	2.35105	1
Injection tuning ν_z	—	2.118	2.1175	1
Straight section quad. strengths	m^{-2}	D = −5.0931	D = −5.0912	1
	m^{-2}	F = 5.4511_5	F = 5.4494_5	1
Perturbator strengths	mrad	P_1 = 2.5243	P_1 = 3.1453	1
	mrad	P_2 = −1.9199	P_2 = −2.0471	1
	mrad	P_3 = 6.1774	P_3 = 7.7272	1
Sextupole strengths (±)	m^{-3}	5.0	6.0	1

cross section of and the coordinate system for the septum at I (Fig. 1) are shown schematically on Figs. 13(a), (b). At E the septum is defined simply by a (positive) x coordinate, given in Table I, and by its thickness (0.002 inch); it is wide in the z-direction and electrostatically bends the beam outwards with a radius curvature of about 25–35 metres (not yet precisely defined).

The sequence of units in the ring, and the lengths of the drift-spaces between them, are (starting at I and proceeding clockwise, i.e. in the beam direction):

I, 5 cm, D, 25 cm, f, 15 cm, H(+), 15 cm, M, 30 cm, P_1, 30 cm, d, 30 cm, f, 20 cm, p.q., 20 cm, M, 30 cm, p_2, 30 cm, d, 25 cm, F, 10 cm, E, 90 cm, D, 20 cm, F, 1.0 m**, D, 25 cm, f, 15 cm, H(−), 15 cm, M, 60 cm, d, 30 cm, f, 20 cm, p.q., 20 cm, M, 60 cm, d, 25 cm, F, 25 cm, P_3, 75 cm*, D, 20 cm, F, 95 cm,

and I follows to complete the ring (codes are as listed above: i.e. as in Fig. 1). The out-of-ring items are at *('M_{en}') and **('M_{ex}'), at positions along the drift space which are yet to be fixed; in Fig. 1 'M_{en}' would lie above the plane of the figure to the right of P_3; 'M_{ex}' would lie in the plane, below the line XW (i.e. outside the ring) and between ($S3$) and ($S4$) quadrupoles. These units have not been designed.

The small differences between Table I and the first ring of Ref. 5 are due to using $\beta = 0.475$ and retuning this ring so that the pulsed-quadrupole strength during ejection lies in a range falling about equally on either side of zero. The use of $5\ m^{-3}$ sextupoles for ring (1) but $6\ m^{-3}$ for the others is somewhat illogical for ring (4), for which the stored beam emittance is relatively large. The nonlinearity due to the sextupoles depends on sextupole strength and beam size; in Ref. 6 the question of reviewing, for ring (4), both the choice of $6\ m^{-3}$ sextupole and the 12 mm injection perturbation is discussed. A 'final' design will have to be chosen in any case when the site is definite; points such as these can be reviewed at that time.

APPENDIX II

Summary of Postulated Tolerances or Required Precisions for Alignment and Energization of Ring Components

The distinction between 'random' and 'systematic' errors and tolerances and other details are fully explained in Sec. 4 of Ref. 6. This includes a 13% upward adjustment employed when random errors are combined, as a best estimate of a conversion factor to 95% confidence values when inputs are specified by a limit-of-error tolerance.

TABLE A-II
Postulated tolerances and precisions

	δx	δz	δs	$\delta\theta$ (tilt)	$\delta\phi$ (twist)
RANDOM displacements	mm	mm	mm	mrad	mrad
Fiducial marks, positioning on unit	0.1	0.1	—	—	included below
Positioning of quadrupole (each end)	0.1	0.1	0.75	0.2	0.5
Positioning of bending magnet	0.1	0.1	(same as δx)	0.2	0.2
SYSTEMATIC: magnets vs quadrupoles	0.1	0.1	0.1	—	—

NOTES: For a 90° bending magnet in the absence of tilt δx at one end is equal to δs at the other; coordinates at magnet centre (as Fig. 4(c)) are not used. The 0.75 mm (0.030 in.) longitudinal positioning error is a compromise value—if fringing end-fields did not overlap 0.5 mm would have seemed reasonable, for units of effective length only 30 cm.

INDICES AND FIELD-STRENGTHS, and properties of ring elements.

Half-lengths of bending magnets, ± 0.1 mm; for quadrupoles, any half-length or pole-spacing errors are corrected for by adjusting field-strengths.
Bending magnet $n = 0.5 \pm 0.003$ (random) or ± 0.0015 (systematic)
Bending magnet $\delta B/B$ (initial precision) $= 10^{-4}$
Quadrupole strength $\delta K/K$ (initial setting) $= 6 \times 10^{-4}$
For final precision (or stability) values, see text; these are most stringent for F and f quadrupoles, less so for bending magnets.
N.B. The above 'limits of error' are taken as $\sqrt{3}$ times the rms errors (see Ref. 6).

Note the systems of coordinates used, indicated by Fig. 4(c), especially the ideas of 'twist' and 'tilt'. We use the term 'tolerances' for values chosen 'a priori' (from experience or similar prior studies) for the probably attainable misalignment limits, and then compute the effects these would cause, although where we can set, from basic ring characteristics, a definite accuracy which should be met, we use the alternative term 'required precision' instead of 'tolerances'. The postulated tolerances used are given in Table A-II.

By contrast to the situation for misalignments, the ring 'tuning' accuracy (in terms of ν_x) is definable and therefore 'required precisions' can be deduced for the magnetic quadrupole fields. A lower precision, the 'initial precision', is acceptable for a setting-up stage (with suitable procedures) so that finally the 'required precisions' emerge as only the degree of stability needed in the current supplies for certain units, and servo-mechanisms may be available to aid their attainment. These are the precision values given in Table A-II for quadrupole fields.

Finally, there is necessarily some uncertainty in how the effects of the various errors are combined. Usually we combine estimates of effects each of which is taken at the 'worst' point around the orbit. There is no assurance that all components will be 'worst' at the same point—indeed this is very unlikely, although x-effects tend to be largest where β_x is large, and z-effects largest where β_z is maximum. The 'quadrature' sums given may be justified, and they may in some cases be felt likely to be pessimistic, because of this; the arithmetic sums shown almost certainly overestimate the expected effects.

APPENDIX III

Quadrupole Imperfections and Maximum Apertures

The field in any practical quadrupole can be described in terms of harmonics. If the poles are similar and symmetrically placed the troublesome harmonics are $n = 6$ and 10 (the fundamental term being $n = 2$) in the equation[11]

$$B_\theta = \sum_{n=1}^{\infty} h_n r^{n-1} \cos n(\theta - \phi_n).$$

Thus, expressed as a fraction of the desired field, the 10th harmonic varies as r^8, and is usually dominant near the outer limit of the aperture; the 6th, varying as r^4, may dominate at radii of $\sim 25\%$ of the aperture radius. The other problem concerns 'aspect ratio', which for our case is near the practical limit, since when pole-tip length and bore are comparable design may be difficult; fringe fields become important and harmonics and other

aberrations in the fringe fields may differ from the defects which dominate in 'long' quadrupoles. From manufacturers' information, for a 7-in. bore design for 30-cm effective length, one model was quoted as having $>1\%$ of 10th harmonic at 75% of bore radius, while for other models $\sim 1\%$ at 90% of bore radius may be attainable. On an r^8-law basis these specifications differ by a factor >4.3. Allowing for difficulties connected with aspect ratio one could perhaps hope to achieve 1% of 10th harmonic at 80% bore radius. A 7 in. quadrupole (bore radius 88.9 mm) with an envelope maximum of 84 mm then corresponds to (for 1% at 80% radius) a 10th harmonic defect of 3.8%. An elementary computation was made to determine what effect a 4% or smaller defect (reduction at maximum envelope position) in the 'worst' quadrupole would produce, using the computer code OSECO[12], and an iterative method. Figure 12 gives the results in the form of the exit beam emittance diagram at the septum. The 'tip' of the ideal emittance triangle for the positive limiting $\Delta E/E$ value taken at the end of extraction (the worst case) has been truncated to allow for the finite septum thickness, and then its position was recomputed with a defect which diminishes the field in the one quadrupole in question during the last orbit only; the new point K_+ is given for 4, 2.5 and 1.5% diminution. In fact the 10th harmonic term may be reduced due to the motion in the vertical direction; for maximum $|z|$ for our conditions (about $\pm 4.5°$ away from an Ox direction) the reduction factor may attain $1/\sqrt{2}$, corresponding to the points labelled 'R' on Fig. 12 (for 4 and 2.5% cases). The thicker line joining these points to K_+ indicates the range within which the distorted emittance diagram apex may lie. It is seen that a 1.5% defect is not a serious matter, but 4% at the aperture in question seems quite undesirable.